Rapid and Precise Analysis of Carbon Dioxide Clumped Isotopic Composition by Tunable Infrared Laser Differential Spectroscopy

Zhennan Wang,[†] David D. Nelson,[‡] David L. Dettman,*[,†] J. Barry McManus,[‡] Jay Quade,[†] Katharine W. Huntington,[§] Andrew J. Schauer,[§] and Saburo Sakai[∥]

[†]Department of Geosciences, University of Arizona, Tucson, Arizona 85721, United States

[‡]Aerodyne Research, Inc., Billerica, Massachusetts 01821, United States

[§]Department of Earth and Space Sciences, University of Washington, Seattle, Washington 98195, United States

[∥]Institute of Biogeochemistry, Japan Agency for Marine-Earth Science and Technology, Yokosuka, Kaganaga 237-0061, Japan

S *Supporting Information*

ABSTRACT: The high precision measurement of doubly substituted ("clumped") isotopologues in CO_2 is a topic of significant interest in isotope geochemistry. Here we describe the performance of a new isotope ratio laser spectrometer using tunable infrared laser differential absorption spectroscopy (TILDAS). The TILDAS instrument has two continuous-wave lasers to simultaneously measure the four isotopologues involved in the $^{12}C^{16}O_2 + {}^{13}C^{16}O^{18}O \rightleftharpoons {}^{13}C^{16}O_2 + {}^{12}C^{16}O^{18}O$ exchange reaction. CO_2 samples are trapped in a low volume (∼250 mL) optical multipass cell with a path length of 36 m. Each sample is compared to a reference gas, and clumped isotopologue precision of 0.01‰ (SE) is achieved within 20 min for 15 μmol samples. Similar precision is also achieved for bulk isotopic composition. The degree of rare isotope clumping in excess of strictly random distribution ($\Delta_{16O13C18O}$) measured by this TILDAS instrument varies linearly with theoretically calculated values and shows a very weak dependence on bulk isotopic composition.
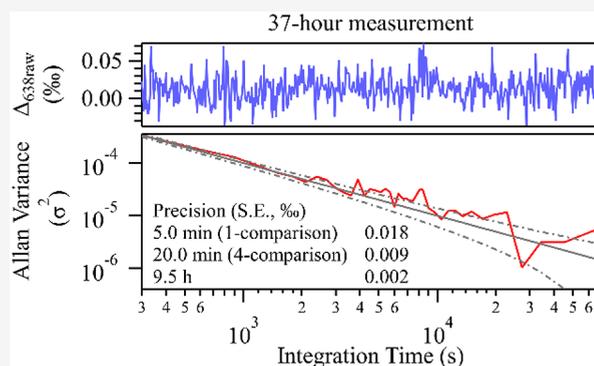
The measurement of rare isotopologues of carbon dioxide has become a topic of significant interest in multiple fields of isotope geochemistry, from geothermometry to tracing sources of CO_2 in the atmosphere. Carbon dioxide clumped isotope thermometry, focused on the formation temperatures of carbonate minerals, is the most developed application of the geochemistry of multiply substituted isotopologues. The degree of heavy (and rare) isotope "clumping" (e.g., $^{16}O^{13}C^{18}O$) beyond an expected random distribution can be related to the temperature of calcite precipitation. This provides an independent temperature estimate that, when combined with carbonate $\delta^{18}O$ values, can constrain paleo-water $\delta^{18}O$ values. Unlike the classic oxygen isotope carbonate−water paleothermometer, this thermometer is based solely on the $^{13}C−^{18}O$ bond ordering in carbonates and requires no assumptions about the $\delta^{18}O$ of water from which carbonates grew.[1,2] Clumped isotope thermometry can also provide a new window into nonequilibrium isotopic fractionations in the laboratory and in nature. Although a nascent field, it is already playing a significant role in a wide range of subjects, such as the following: terrestrial and marine paleoclimate;[3,4] paleoaltimetry, structural geology, diagenesis, and basin thermal histories;[5,6] thermal histories of meteorites;[7]

thermochronology and geobarometry;[8,9] vital effects;[10,11] physiology of extinct fauna.[12]

However, a major challenge for carbonate clumped isotope thermometry is the difficulty of the measurement, due to the extremely low natural abundance and subtle variation with temperature of clumped isotopologues. Virtually all laboratories today use isotope ratio mass spectrometry (IRMS) for clumped isotope thermometry, where measurements typically require extensive sample purification, 2−4 h of machine time per sample, replication of these analyses, sample sizes of 30 μmol or greater, and analysis of many reference carbon dioxide gases and carbonate standards to achieve usefully precise data.[13−16] Moreover, the clumped isotope values rely on $\delta^{13}C$ and $\delta^{18}O$ measurements that must be corrected for ^{17}O mass interference, because both the $^{13}C^{18}O^{16}O$ and $^{12}C^{18}O^{17}O$ molecules have the same cardinal mass of 47 AMU. This correction is based on an assumed $^{17}O−^{18}O$ abundance relationship, whose variability in nature may introduce significant errors in clumping estimates.[17,18]
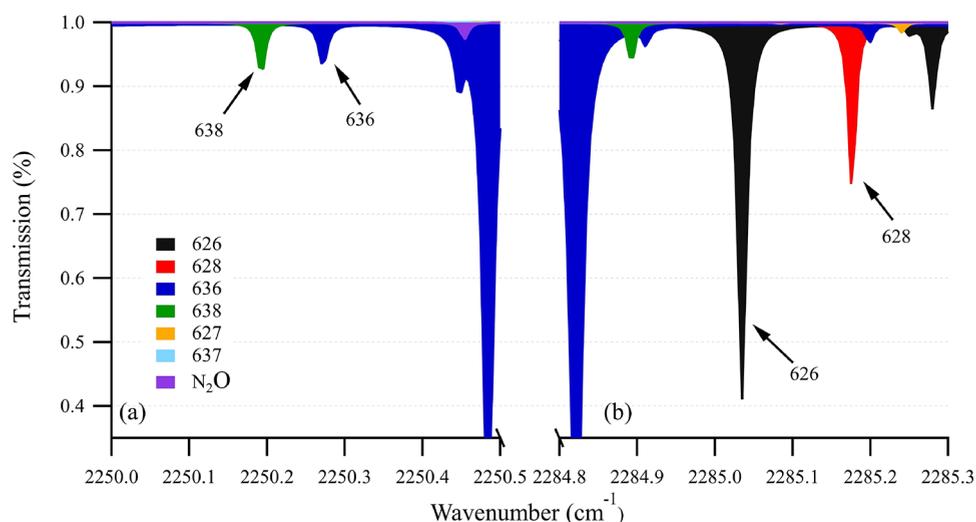
Figure 1. Absorption line position and simulated transmission coefficient for four isotopologues of carbon dioxide using the HITRAN database. (a) Laser 1 at 2250.2 cm^{-1} region. (b) Laser 2 at 2285.1 cm^{-1} region. The simulation was conducted at a concentration of 0.35% (balance nitrogen), a pressure of 60 Torr, and a path length of 36 m. The selection of concentration and pressure is explained in TILDAS Instrument Stability. Nitrous oxide was added to the simulation due to its potential impact on the spectral region of interest.

More efficient, direct, and broadly applicable clumped isotope measurements can potentially be achieved by laser spectroscopy, which uses an infrared laser to measure the absorption spectrum of the molecules of interest. Laser spectroscopy is now commonly used for measurement of $\delta^{18}O$ and δD compositions in water and is commercially available for $\delta^{18}O$ and $\delta^{13}C$ analysis in carbon dioxide.[19,20] Laser methods have recently been developed for high-precision $\delta^{17}O$ analysis in water[21,22] as well as for clumped isotopes of methane.[23,24] Our recent work[25−27] and that of Prokhorov et al.[28] have demonstrated the great promise of tunable infrared laser differential absorption spectroscopy (TILDAS) for clumped isotope measurements of carbon dioxide. In this paper, we describe the development of a new dual-laser TILDAS instrument and associated sampling system that provides high precision and rapid measurements of the clumped isotopic composition of carbon dioxide. This TILDAS instrument improves upon a prototype instrument[29] built by Aerodyne Research, Inc., allowing simultaneous and direct measurement of all four carbon dioxide isotopologues of interest. The sampling system makes use of a working reference gas to correct for instrument drift, which ensures long-term stability and allows long integration times for sample measurement. Through recent improvements in laser design and sample handling described in this paper, we can routinely achieve precisions of 0.01‰ (1 SE, standard error, $n = 4$) using our new isotope ratio laser spectrometer, comparable to precisions using well-established IRMS techniques. Moreover, our average measurement time of 20 min and sample size requirement of 15 μmol of CO_2, or 1.5 mg of calcite equivalent, are significantly shorter and smaller than that of well-established IRMS techniques.

■ EXPERIMENTAL SECTION

Laser-Specific Notation. In clumped isotopes geochemistry, the variable Δ_i is used to describe the abundance of isotopologue i relative to that expected if all isotopes are randomly distributed (stochastic distribution) among all isotopologues,

$$\Delta_i = \left(\frac{R_i}{R_{i-r}} - 1 \right) \times 1000 \tag{1}$$

where R_i is the abundance ratio of an isotopologue of interest (i.e., i) relative to the isotopologue having no rare isotopes (i.e., $^{12}C^{16}O^{16}O$), and subscript r in R_{i-r} stands for the random distribution condition. The isotope exchange reaction involving one doubly substituted isotopologue $^{13}C^{18}O^{16}O$ can be written as

$$^{12}C^{16}O^{16}O + {}^{13}C^{18}O^{16}O \rightleftharpoons {}^{12}C^{18}O^{16}O + {}^{13}C^{16}O^{16}O \tag{R1}$$
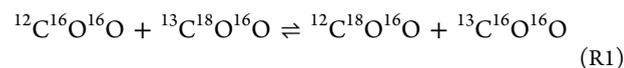
and the temperature-dependent equilibrium constant K for this reaction is expressed as

$$K = \frac{[^{12}C^{18}O^{16}O][^{13}C^{16}O^{16}O]}{[^{12}C^{16}O^{16}O][^{13}C^{18}O^{16}O]} \tag{2}$$

A decrease in temperature drives the reaction to the left, increasing the abundance of $^{13}C^{18}O^{16}O$. Wang et al.[30] derived the relationship between $\Delta_{13C18O16O}$ and K:

$$\Delta_{^{13}C^{18}O^{16}O} \approx -1000 \ln \frac{K}{K_r} \tag{3}$$

where K_r is the equilibrium constant for the fully randomized stochastic distribution. in reaction R1, K_r equals 1.

Each of the four isotopologues in eq 2 can be measured directly by the TILDAS instrument in a carefully chosen spectral region. In this study, we introduce a new notation for clumped isotopes of CO_2, Δ_{638}, in recognition of the uniquely different way we are making the measurement by TILDAS. This laser-specific notation is based on the Air Force Geophysics Laboratory (AFGL) shorthand notation which has been used in the HITRAN database[31] for decades. Here $^{16}O^{12}C^{16}O$, $^{16}O^{13}C^{16}O$, $^{16}O^{12}C^{18}O$, and $^{16}O^{13}C^{18}O$ are referred to as CO_2 626, 636, 628, and 638, respectively. Isotopologues are identified by the second digit of the atoms' atomic mass. This Δ_{638} term is different from the Δ_{47} term used in IRMS measurement of clumped isotope because there is no isobar interference using TILDAS.[30] For this study, we will report our

Table 1. Parameters for Four Isotopologue Lines of Carbon Dioxide

isotopologue (AFGL notation)	frequency (cm^{-1})	line intensity (cm^{-1} /(molecule × cm^{-2}))	lower-state energy (cm^{-1})	ΔE (cm^{-1})
626	2285.030	6.055×10^{-22}	2075.7	
628	2285.171	2.083×10^{-22}	1052.8	1022.9
636	2250.267	5.675×10^{-23}	1347.9	
638	2250.188	6.446×10^{-23}	154.6	1193.3

results relative to a working reference gas (WR), which corrects the TILDAS instrument drift during measurement, rather than relative to K_r, and eq 3 then becomes

$$\Delta_{638raw} = -1000 \ln \frac{K}{K_{WR}} \tag{4}$$

where Δ_{638raw} is defined as the Δ_{638} value of the sample gas with respect to the working reference gas.

In contrast to IRMS, each isotopologue can be measured specifically using TILDAS, we define isotopologue composition as

$$\delta_i = \left(\frac{\frac{[i]_{sample}}{[626]_{sample}}}{\frac{[i]_{standard}}{[626]_{standard}}} - 1 \right) \times 1000 \tag{5}$$

where i = 636, 628, and 638. In the more common situation in which the isotopes are not stochastically distributed among the isotopologues, δ_{636} and δ_{628} are good approximations of bulk isotopic composition, $\delta^{13}C$ and $\delta^{18}O$, respectively, whereas δ_{638} is approximately equal to ($\delta_{636} + \delta_{628}$), and thus to ($\delta^{13}C + \delta^{18}O$).

Selection of Absorption Lines. Two lasers are used to measure the four isotopologues of CO_2 (626, 636, 628, and 638) drawn from the HITRAN database (Figure 1; Table 1). The spectral region of 2250.2 cm^{-1} was chosen for $^{13}C^{18}O^{16}O$ and $^{13}C^{16}O_2$ lines, which are free from spectral interference. The absorption lines for $^{12}C^{16}O_2$ and $^{12}C^{18}O^{16}O$ were selected in the 2285.1 cm^{-1} region because of the comparable line intensity (Table 1). Therefore, all four isotopologue lines can be simultaneously measured at the same conditions, i.e., concentration, pressure, path length, which is critical to shorten the measurement time and consequently minimize instrumental drift.

The calculation of equilibrium constant K in eq 2 can be manipulated to yield an equivalent combination of isotopologue ratios that match the peak pairs in each laser:

$$K = \frac{[628][636]}{[626][638]} = \frac{[628]}{[626]} \bigg/ \frac{[638]}{[636]} \tag{6}$$

where the isotopologue ratios $[638]/[636]$ and $[628]/[626]$ are absorption peak ratios measured in the absorption windows of the two lasers. Absorption peaks can respond strongly to changes in temperature and pressure, so each variable must be controlled and carefully monitored. However, the approach used in eq 6 uses a ratio of peak ratios, $[638]/[636]$ and $[628]/[626]$, that have similar lower-state energy differences (Table 1, ΔE, 1023 vs 1193 cm^{-1}), which reduces the impact of temperature change in the instrument. This is because the temperature impact on absorption intensity is similar for the peaks measured in each laser, leading to a cancelation or reduction in the effects of temperature-dependent line intensities on the equilibrium constant K measurement.

TILDAS Instrument. Our newly designed TILDAS instrument is a dual-laser spectrometer based on Aerodyne's commercial atmospheric CO_2 stable isotope analysis instrument[19] and on a prototype CO_2 clumped-isotope instrument.[29] The basic instrument design is described in the previous publications.[20,23,24,29] In our new instrument, two lasers are used to measure the four isotopologues of interest. An interband cascade laser (laser 1, Nanoplus, Germany) is tuned to 2250.2 cm^{-1} to measure 636 and clumped-isotopologue 638, and a quantum cascade laser (laser 2, Alpes Laser, Switzerland) is tuned to 2285.1 cm^{-1} to measure 626 and 628.

The lasers are housed in a pair of atmospherically sealed, thermoelectrically cooled containers. The supply voltages to the lasers are cycled at 1.6 kHz to rapidly scan the laser frequency across 350 channels for laser 1, 450 channels for laser 2, and 60 channels for laser shutoff to measure zero-light level, providing 96 000 peak-area measurements of each CO_2 isotopologue per minute. The laser light is collimated and combined into a single beam which is coupled into an astigmatic multipass absorption cell with a volume of approximately 250 mL and a path length of 36 m.[32] The optical sample cell is made of aluminum and plated with nickel. The cell temperature is recorded by a 30 KΩ thermistor, and cell pressure is monitored by a capacitance manometer (100 Torr full scale, MKS, USA). The cell leak rate is approximately 0.02 Torr/h (at a pressure of 1 Torr), which is negligible for the duration of one measurement subcycle (ca. 5 min). The laser output is captured by a thermoelectrically cooled photovoltaic (HgCdTe) detector. The above optics are all aligned in a temperature-controlled box which is purged with nitrogen gas. The "TDLWintel" software is set up to operate the TILDAS instrument and analyze the absorption spectra in real-time.[33]

Automated Sampling Methodology and System. Like dual-inlet IRMS, comparison to a working reference gas is used to account for instrument drift (eq 4). Each sample measurement is interleaved between two working reference measurements, thus allowing for instrument drift correction along a sequence of sample analysis. To realize this approach, a sampling system (Figure 2) was designed and coupled to the TILDAS instrument, and corresponding control features were developed in the TDLWintel software. The sampling system is composed of electronic valves (Parker, USA), pneumatically driven valves (Swagelok, USA), a capacitance manometer (1000 Torr full scale, MKS, USA), two critical orifices (O'Keefe Controls, USA), and a dry scroll pump (Agilent, USA). All parts are connected by Swagelok fittings and 1/4–1/2″ stainless-steel tubing. The working reference/sample gas is introduced into an intermediate volume of approximately 25 mL to a designated pressure and then expanded into the optical sample cell for measurement. Two electronic valves provide fast-response (~ms) for gas volume and pressure controls. Otherwise, seven pneumatically driven valves
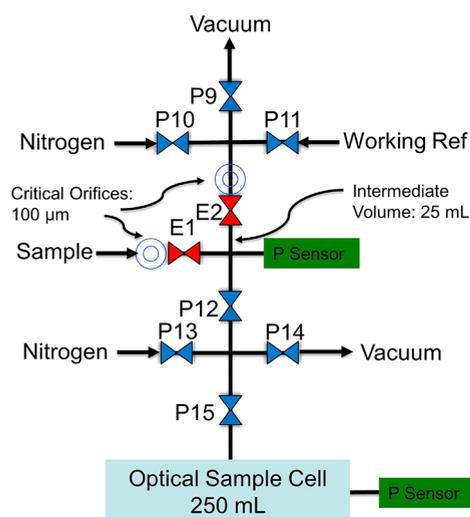
Figure 2. A schematic diagram of the sampling system installed in the TILDAS instrument. E# and P# stand for electronic and pneumatic valves, respectively, and numbers 1−8 were reserved for electronic valves. Concentric circles: critical orifice. P sensor: pressure sensor.

(Swagelok, USA) are used to avoid thermal instability caused by heat generated by electronic valves. To achieve precise, repeatable, and unfractionated gas introduction, the gas flow rate of working reference/sample is restricted by a pair of critical orifices. Between sample and working reference switching, the intermediate volume and optical sample cell are flushed with nitrogen.

Working Reference and Samples. In the practical measurement, the sample and working reference are very likely to have different values in bulk $\delta^{13}C$, $\delta^{18}O$, and in clumped isotopologue value Δ_{638raw}. To mimic this scenario, an uncharacterized carbon dioxide gas was used as the working reference gas in this study, mixed with nitrogen in a stainless-steel canister (Restek, USA) to a concentration of 0.35%. The addition of nitrogen to the carbon dioxide broadens the absorption lines slightly, which improves the precision of the peak area calculation.

The carbon dioxide sample gases were prepared at Isolab, the University of Washington, by equilibrating carbon dioxide that originated from corn fermentation or fossil fuel combustion in pyrex break-seals with South Pole ice core water or evaporatively enriched water held at 4 °C, 22 °C, and 60 °C (equilibration time at least 2 weeks). After the samples were fully equilibrated, the water was removed from the sample to stop isotopologue reordering. Each temperature should therefore lead to a measurable difference in the Δ_{638raw} value. This also creates a broad range in bulk isotopic composition in the CO_2, with a δ_{638raw} range, roughly equal to (δ_{636raw} + δ_{628raw}), of approximately 100‰. In addition, both CO_2 gases were heated in a quartz break-seal in a muffle furnace to 1000 °C overnight. As with the working reference gas, each sample gas was mixed with N_2 in a stainless-steel canister to a concentration of 0.35%. Single-stage stainless-steel regulators (Airgas, USA) were used to control the supply pressure of the sample and reference gases to the inlet system.

Isotopologue Fractionation Investigation. The CO_2/N_2 gas mixtures, i.e., both the sample gases and working reference gas, are stored in stainless-steel canisters before conducting TILDAS measurements. As described above, the CO_2/N_2 mixture gas is introduced into an optical sample cell

through a sampling system that is composed of pressure regulators, pneumatical valves, electronic valves, critical orifices, and stainless-steel tubing. The output pressure of the regulators and critical orifice size were all carefully selected to avoid isotopologue fractionation as the gases are moved through the system. In addition, turbulent gas expansion (Figure 2, from the intermediate volume to the optical sample cell) was also counted on to eliminate isotopic fractionation during gas transfer. To investigate potential fractionation risk across a range of sample conditions, a series of experiments was conducted across multiple settings in gas mixture pressure, pressure regulator output pressure, and critical orifice size.

■ RESULTS AND DISCUSSION

TILDAS Instrument Stability. The original flow-through optical cell of the Aerodyne CO_2 isotope instrument has been retrofitted with vacuum fittings, resulting in a leak-tight optical cell suitable for static sample measurement at various pressures. A 0.35% CO_2 in N_2 was used to test the performance of the instrument, and the pressure for optimal absorption and stability in the TILDAS instrument was found in the 50 to 60 Torr range (Figure s1(a) in Supporting Information). Larger sample sizes (i.e., higher sample pressure) did not significantly improve performance. The volume of sample needed in the TILDAS instrument for a single aliquot or replicate measurement of a sample gas is approximately 310 mL, which includes the optical sample cell, intermediate volumes, and tubing. This leads to a single replicate sample size of 3 to 4 μmol of CO_2, or 0.3 to 0.4 mg of calcite equivalent. The measurement precision in terms of standard error is improved as expected by averaging multiple data points (Figure s1(b) in Supporting Information). Measuring multiple replicates and/or collecting multiple data points in each replicate increases measurement precision but also requires more sample consumption and longer analysis time. However, to achieve high precision measurements and counter the effects of instrument drift, multiple aliquots of the sample gas must be measured. Thus, there is a trade-off between measurement precision, integration time, and sample size.

To test the instrument stability, the Δ_{638} value of a CO_2/N_2 mixture gas at a concentration of 0.35% was continuously monitored for 8 h at a pressure of 60 Torr. Typical instrument drift and corresponding Allan variance plot of Δ_{638} are shown in Figure 3. The 1-s Allan deviation of 0.127‰ is consistent with that depicted in Figure s1(b), whereas the minimum Allan deviation of 0.013‰ is obtained with an integration time of 240 s. The instrument drift becomes significant over an integration time longer than approximately 400 s. This indicates that one measurement subcycle, which includes both a single sample replicate measurement and a single working reference measurement, should be at least 240 s to collect as many data points as possible before drift becomes significant but less than 400 s to avoid instrument drift effects. Based on extensive testing, a measurement cycle of 5 min was determined as the optimal balance between measurement precision, instrument drift, and sample size.

Although the overlap between $^{12}C^{18}O^{16}O$ and the small $^{13}C^{16}O_2$ peaks in the region of 2285.1 cm^{-1} (laser 2) could complicate our measurements, this peak is very precisely constrained based on the $^{13}C^{16}O_2$ abundance measured at 2250.267 cm^{-1} (using laser 1). The latter peak, which is free from interference and has a stronger line intensity, is used to quantify $^{13}C^{16}O_2$, and the TDLWintel software removes a
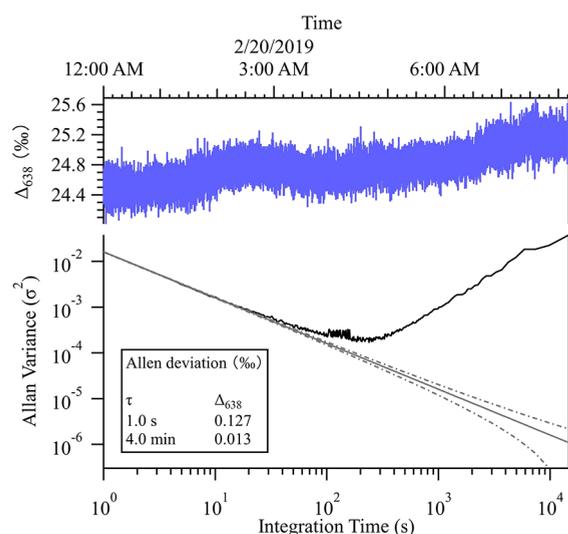
Figure 3. Upper panel: typical instrument drift in Δ_{638} measurement over 8 h. Lower panel: Allan variance plot of Δ_{638} with a theoretical simulation of white noise (gray and dotted lines). The inset shows Allen deviations at integration times of 1 s and 4 min.

Figure 4. Upper: Δ_{638raw} of sample gas against working reference gas over 37 h using 5 min sample-reference gas measurement cycles. Lower: Allan variance plot.

proportional peak area from the combined peaks at 2285.1 cm^{-1} to quantify the $^{12}C^{18}O^{16}O$ peak for spectral fitting. This approach has proved to be robust across a range of $\delta^{13}C$ and $\delta^{18}O$ values in CO_2 samples.

Measurement Protocol and Long-Term Precision. A proof-of-concept study was conducted to investigate the feasibility of a working reference gas concept in the TILDAS instrument. The CO_2/N_2 sample and working reference gases were made in two identical stainless-steel canisters (Restek, USA) with the same concentration of 0.35%. A basic analytical protocol was established as follows:

(1) Introduce working reference into the intermediate volume of approximately 25 mL to designated pressure;

(2) Expand working reference into the optical sample cell and measure working reference for ∼100 s;

(3) Pump out the intermediate volume and introduce the sample to the designated pressure while measuring the working reference;

(4) Pump out the optical sample cell, flush with dry nitrogen, and pump out the nitrogen;

(5) Expand the sample into the optical sample cell as in 2 above and conduct measurement of sample for ∼100 s;

(6) Repeat steps 1−5 to obtain the required number of measurement subcycles.

The Δ_{638raw} value of sample gas against working reference gas was measured for over 37 h, using a measurement subcycle of 5 min for one comparison of the reference gas and the sample gas (Figure 4). The Allan variance plot in Figure 4 illustrates that the instrument drift is successfully canceled out of the measurement through the use of a working reference gas, and the variability of Allan variance (σ^2) appears to show a declining trend obeying an ideal statistical-noise-limited behavior as the measurement proceeds. By measuring four subcycles using 20 min total time, the precision of this TILDAS instrument on CO_2 clumped isotope Δ_{638raw} measurement after the incorporation of working reference gas was improved to ±0.009‰ (SE, n = 4). With four measurement subcycles of the sample gas, the total sample size
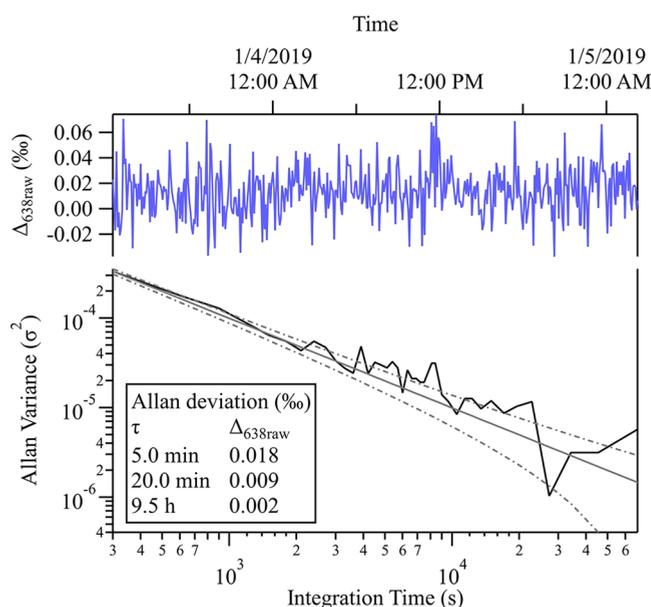
needed was approximately 15 μmol of CO_2, or 1.5 mg of calcite equivalent.

Measurement of Heated and Equilibrated CO_2 Gases. Following the analytical protocol described above, eight sample gases were analyzed with respect to a working reference gas. These are the CO_2 samples equilibrated at different temperatures described above. Each sample was measured twice (Table s1 in Supporting Information, test 1 and test 2) with an interval of 8 h between measurements during which the sample remained in the canister. Four subcycles were averaged to obtain one individual meaningful measurement with a targeted precision of 0.01‰. The results show that the two test results agree with each other, which is very encouraging in that Δ_{638raw} values were measured with high internal precision (1 SE < 0.01‰) across an 8-h time interval. In addition, δ_{636raw} and δ_{628raw} values show similar precision (0.02‰, 1 SD), and these ratios will be used to precisely determine $\delta^{13}C$ and $\delta^{18}O$ values of the sample CO_2 after calibration to standard materials. This minimizes the concern over clumped isotope reordering due to the usage of a dry scroll vacuum pump and canisters made of stainless steel, where the presence of adsorbed water on the container surface could be a significant concern.[34] Note that clumping reordering was observed in only one heated CO_2 sample; this is discussed in Supporting Information.

The reported TILDAS results are proportional to the theoretical equilibrium Δ_{638} values from Petersen et al.[35] (Figure 5). We used an approach analogous to the absolute reference frame of Dennis et al.,[14] or carbon dioxide equilibrium scale (CDES), for normalizing IRMS clumped CO_2 measurements to theoretical equilibrium Δ_{47} values.[30] The theoretical difference in clumping between 4 °C and 1000 °C samples is expected to be 1.048‰, whereas that reported by TILDAS in fermented corn and fossil fuel CO_2 samples is 1.073‰ and 1.144‰, respectively. Interestingly, this shows that the TILDAS instrument exhibits a slightly expanded scale, such that the TILDAS measurement precision of <0.01‰ will
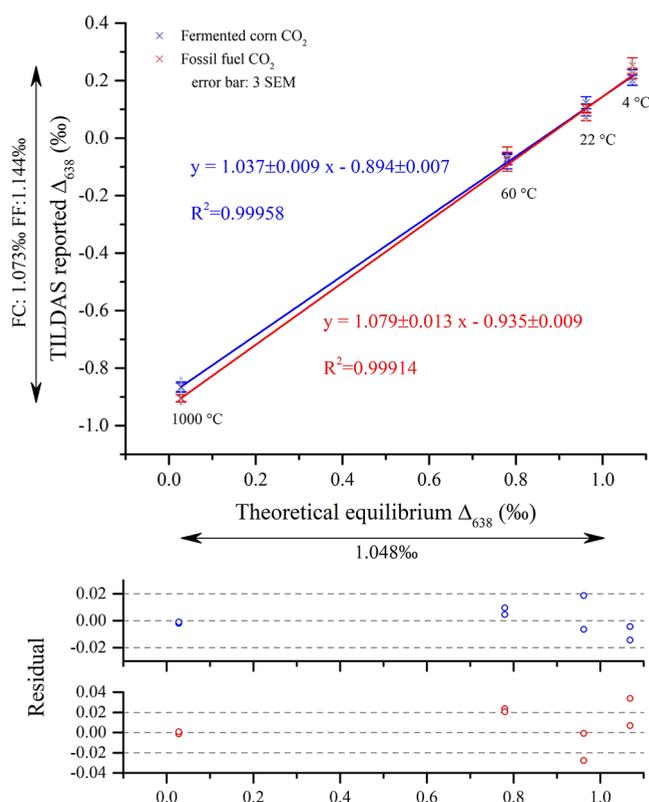
Figure 5. Reported TILDAS Δ_{638raw} values versus theoretical equilibrium CO_2 Δ_{638} values. Numbers and symbols in blue: fermented corn CO_2; in red: fossil fuel CO_2. Residuals for either gas, below, do not show a trend.

be further improved when the measured Δ_{638} values are converted to the CDES.[14]

Equilibration of CO_2 with water resets the clumping in the CO_2 to a value that is controlled by temperature, and each of the gases equilibrated at the same temperature therefore should have identical Δ_{638} values (Figure 5). Although the values produced in this test are not identical for each temperature, they are very similar (Figure 6). This implies that there is minimal to insignificant dependence on the bulk isotopic composition in the measurement of Δ_{638raw} values. If a single average slope is calculated based on the 4 °C, 60 °C, and
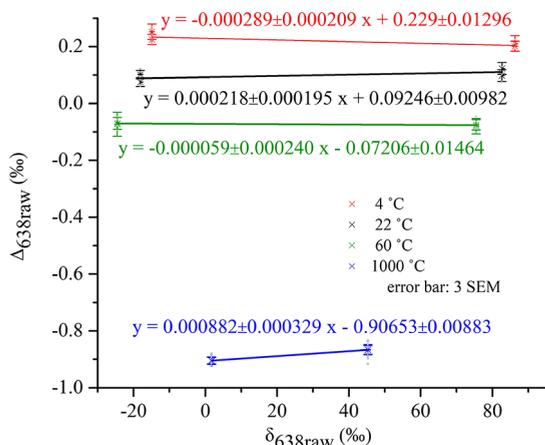
Figure 6. Observed relationship between Δ_{638raw} and δ_{638raw} in the heated and equilibrated gases using TILDAS instrument.

1000 °C lines, we obtain -6.23×10^{-5}, with intercepts of 0.22447, -0.07291, and -0.88429, respectively. Using this slope, the temperature of sample equilibrated at 22 °C can be calculated as a quality control assessment,[14] which results in 25 $\pm$ 4 °C (1 SD). Additional testing is needed to determine if the variance in observed slopes in Figure 6 is due to noise in our first set of measurements or whether this is systematic. The relatively weak correlation between Δ_{638raw} and δ_{638raw} demonstrated in this preliminary study is very encouraging, in that it implies that working reference gases (which almost always show clumping associated with room temperature equilibration with water vapor) can have bulk isotopic compositions that are significantly different from the sample compositions without strongly affecting the Δ_{638raw} measurement.

Testing Isotopic Fractionation during Sample Handling. Compared to IRMS, the carbon dioxide sample handling and analysis technique are very different in the TILDAS approach. The TILDAS instrument and sample inlet system were operated across a range of conditions to investigate potential fractionation risk, especially due to the usage of critical orifices, regulators, large-diameter tubing (1/4−1/2″), and storage canisters. Three working references with the same concentration of 0.35% CO_2 in N_2, i.e., WR1, WR2, and WR3, were made and stored in three canisters. There were small differences in the final Δ_{638} values of these three gases resulting from the preparation process and perhaps from slight differences in the final concentration of CO_2 (e.g., WR1 0.346% and WR2 0.354%). We varied our sample handling procedures systematically in an attempt to isolate potential artifacts. The experimental parameters and results are summarized in Table 2.

Experiments 1 and 2 (expt 1 and expt 2) compared differences in the size of the critical orifices used to restrict sample flow. Both were 100 μm in expt 1, and one was increased to a diameter of 125 μm in expt 2. The TILDAS-reported Δ_{638raw} values suggest that the usage of different sizes of critical orifices did not cause an observable fractionation because (1) the result is comfortably within the uncertainty range of zero enrichment in both cases, and (2) expt 1 result agrees with expt 2. Analogously, the results of expt 3 and expt 4 indicate that no observable fractionation was caused by a significant increase in regulator output pressure (5 vs 15 psig).

Experiment 5 was conducted to investigate the possible occurrence of fractionation in the gas stored in a canister and throughout a prolonged (11 h) measurement of Δ_{638}. Before WR3 was introduced into the TILDAS instrument, some of it was pumped away for 30 s (analogous to the gas consumption of three subcycles) through the sample critical orifice, valve E1, P12, and P14 (Figure 2). This reduced the amount of total gas in WR3 relative to WR1, leading to a large difference in the proportional rate of consumption of the two gases with the WR3 gas being depleted much more rapidly than WR1. Figure 7(a) shows the continuous variation of Δ_{638raw} (WR3 vs WR1) values over 11 h until WR3 ran out, during which the isotopic composition did not change as WR3 was consumed. In summary, the above experiments demonstrate that no observable fractionation occurs within the sampling system and TILDAS instrument.

Cancelation of Diffusion Effects on Δ_{638} Ratio. Using Chapman−Enskog theory, the diffusion coefficient of gas a through gas b can be expressed as

Table 2. Summary of Experimental Conditions and Results Regarding Potential Isotopic Fractionation Investigation[a]

experiment no.	gas no.	regulator output pressure (psig)	critical orifice diameter (μm)	Δ_{638raw} (‰) mean ± 1 SE	δ_{636raw} (‰) mean ± 1 SE	δ_{628raw} (‰) mean ± 1 SE
expt 1	WR1	5	100	−0.004 ± 0.005	0.005 ± 0.003	−0.002 ± 0.002
	WR1	5	100			
expt 2	WR1	5	100	0.003 ± 0.006	0.021 ± 0.003	0.014 ± 0.002
	WR1	5	125			
expt 3	WR1	5	100	−0.035 ± 0.003	0.047 ± 0.003	0.071 ± 0.002
	WR2	5	100			
expt 4	WR1	5	100	−0.037 ± 0.004	0.050 ± 0.003	0.058 ± 0.002
	WR2	15	100			
expt 5	WR1	5	100	−0.021 ± 0.003	0.043 ± 0.001	0.017 ± 0.001
	WR3	5	100			

[a]In experiment 2 (expt 2), the regulator output pressure of WR1 was set to 5 psig, and it was connected to both the sample inlet (critical orifice diameter of 100 μm) and the working ref inlet (critical orifice diameter of 125 μm). In expt 4, WR1 was connected to the sample inlet and its regulator output pressure was set to 5 psig. WR2 was connected to the working ref inlet, and its regulator output was 15 psig. Both critical orifices had a diameter of 100 μm.

$$D \propto \sqrt{1/\mu} \tag{7}$$

where μ is the reduced mass given by $\mu = m_a m_b/(m_a + m_b)$. In this study, carbon dioxide is mixed with nitrogen for clumped isotope measurement, and two isotopologue ratios, [638]/[636] and [628]/[626], are independently measured by two lasers, such that the diffusion coefficient ratios can be calculated as

$$\frac{D_{638}}{D_{636}} = \frac{\sqrt{\frac{45 \times 28}{45 + 28}}}{\sqrt{\frac{47 \times 28}{47 + 28}}} = 0.991806$$

$$\frac{D_{628}}{D_{626}} = \frac{\sqrt{\frac{44 \times 28}{44 + 28}}}{\sqrt{\frac{46 \times 28}{46 + 28}}} = 0.991510 \tag{8}$$

while the diffusion coefficient ratio of four isotopologues used to calculate the equilibrium constant K is

$$\frac{D_{628} D_{636}}{D_{626} D_{638}} = \frac{\sqrt{\frac{44 \times 28}{44 + 28}} \sqrt{\frac{47 \times 28}{47 + 28}}}{\sqrt{\frac{45 \times 28}{45 + 28}} \sqrt{\frac{46 \times 28}{46 + 28}}} = 0.999702 \tag{9}$$

Equation 9 shows that the fractionation due to the different diffusion coefficients among the CO_2 isotopologues would result in a deviation of 0.3‰ in Δ_{638}, which is 28 times less than that in the [638]/[636] and [628]/[626] ratios (eq 8). This implies that diffusional fractionation in CO_2 would lead to large changes in bulk $\delta^{13}C$, $\delta^{18}O$ but only small changes in Δ_{638} because of diffusion cancelation. In this study, no observable fractionation in the [638]/[636] and [628]/[626] ratios was found. For example, Figure 7(b) demonstrates that the [628]/[626] ratio remained constant in terms of δ_{628raw} (WR3 vs WR1) values while the WR3 gas was depleted at a significantly faster rate than WR1. In practice, two features help to reduce the isotope fractionation caused by diffusion: (1) the carbon dioxide and nitrogen are well-mixed before being introduced into the sampling system, and (2) turbulent mixing during the gas expansion assists in homogenizing the mixture.

■ CONCLUSION AND FUTURE WORK

We have developed an isotope ratio laser spectrometry method to precisely determine the carbon dioxide clumped isotopic composition, Δ_{638}, using a TILDAS instrument. In addition, this system can rapidly measure the stable oxygen isotope composition, δ_{628}, and stable carbon isotope composition, δ_{636} (both terms are relatable to conventional $\delta^{18}O$ and $\delta^{13}C$ after calibration), at high precision. The TILDAS instrument directly and simultaneously measures four isotopologues, $^{16}O^{12}C^{16}O$, $^{16}O^{13}C^{16}O$, $^{16}O^{12}C^{18}O$, and $^{16}O^{13}C^{18}O$, in the mid-infrared spectral regions of 2250.2 and 2285.1 cm^{-1}. One aliquot measurement yielded a precision of 0.02‰ (1 SE, 5 min) in Δ_{638raw} values (with respect to an uncharacterized working reference gas). With a specially designed sampling system, the concept of which is adapted from dual-inlet IRMS, long-term instrument drift was corrected by using a working reference gas. A precision of 0.01‰ was achieved with four repeated measurements within 20 min, and the total sample size needed was approximately 15 μmol of CO_2, or 1.5 mg of calcite equivalent. With enough sample, additional comparisons will improve the precision of the measurement and ±0.002‰ (1 SE) can be achieved in 10 h (Figure 4). Heated CO_2 samples and samples equilibrated with water at different temperatures demonstrate that the TILDAS Δ_{638raw} values match theoretical values in a linear relationship, at a slightly expanded scale. A weak dependence of Δ_{638raw} on δ_{638raw} was observed with a slope of −0.0003 to 0.0002 over a range of 100‰ in δ_{638raw}, and heated CO_2 samples had a slope of +0.0009 over a 45‰ range of δ_{638raw}. This suggests that accurate measurements of samples across a broad range in bulk isotopic composition should be feasible with only a few working reference gases spanning that range.

Work with this TILDAS instrument is ongoing, including additional calibration efforts and improvements to the TILDAS instrument. Calibration work includes (A) comparison to the international carbonate reference materials NBS-19, NBS-18, and IAEA-603, as well as (B) the clumped isotope interlaboratory comparison carbonates, ETH-1, ETH-2, ETH-3, and ETH-4,[16] and (C) measurement of more carbon dioxide equilibrium scale gases. In addition we are (D) developing
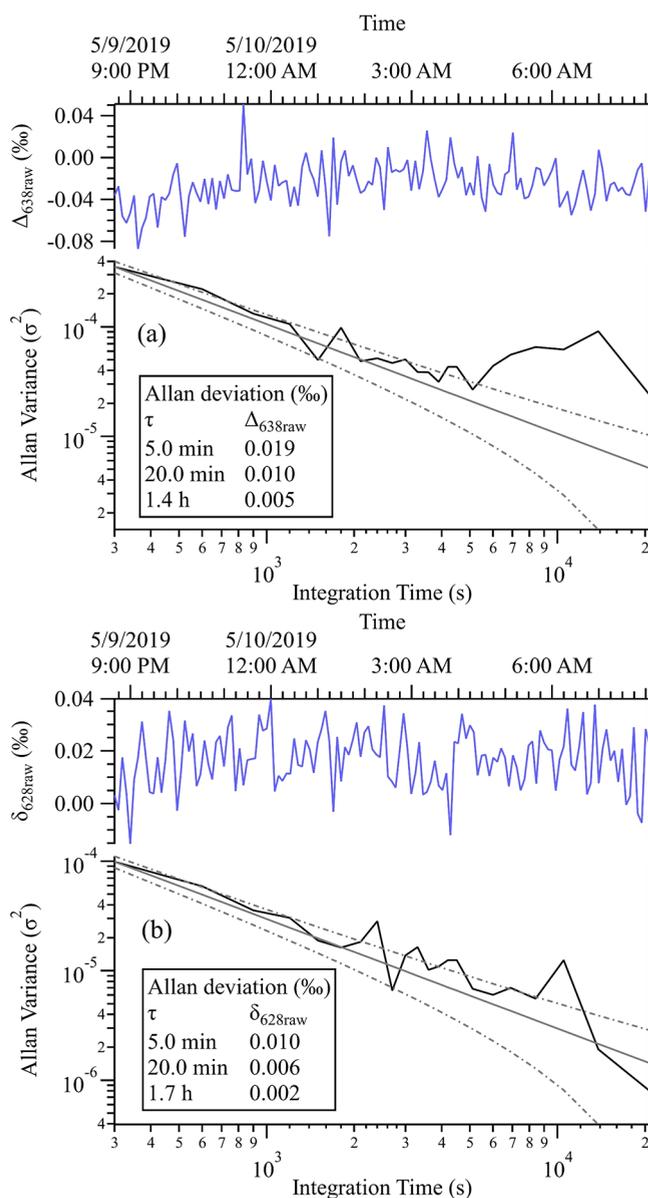
Figure 7. Δ_{638raw} (a) and δ_{628raw} (b) values of one working reference (WR1) with respect to another (WR3) over 11 h and corresponding Allan variance plots. The WR3 was depleted at a faster rate than WR1.

TILDAS instrument thermometry relationships in carbonates using newly created synthetic calcites as well as those already included in publications.[36] These four exercises are the four pillars of IRMS clumped isotope measurement and will be necessary to cross calibrate TILDAS-based Δ_{638} and IRMS-based Δ_{47} measurements. The performance of the TILDAS instrument demonstrated in this study is competitive with the best IRMS systems and surpasses typical IRMS measurements in several key respects, especially in measurement duration, which is typically 20 min or less.

ASSOCIATED CONTENT

ⓢ Supporting Information

The Supporting Information is available free of charge at https://pubs.acs.org/doi/10.1021/acs.analchem.9b04466.

Figure s1. Determine optimal conditions in terms of TILDAS instrument stability. Figure s2. One clumped isotope reordering case. Table s1. Δ_{638raw}, δ_{636raw}, and δ_{628raw} measurement results using a TILDAS instrument (PDF)

AUTHOR INFORMATION

Corresponding Author
*E-mail: dettman@arizona.edu.

ORCID ⓘ
Zhennan Wang: 0000-0001-7772-2026
Saburo Sakai: 0000-0002-3809-0254

Notes
The authors declare no competing financial interest.

REFERENCES

(1) Eiler, J. M. *Earth Planet. Sci. Lett.* **2007**, *262* (3−4), 309−327.
(2) Schauble, E. A.; Ghosh, P.; Eiler, J. M. *Geochim. Cosmochim. Acta* **2006**, *70* (10), 2510−2529.
(3) Eiler, J. M. *Quat. Sci. Rev.* **2011**, *30* (25−26), 3575−3588.
(4) Affek, H. P. Clumped Isotope Paleothermometry: Principles, Applications, and Challenges. In *Reconstructing Earth's Deep-Time Climate-The State of the Art in 2012, Paleontological Society Short Course*; Ivany, L. C., Huber, B. T., Eds.; Paleontological Society, 2012; pp 101−114.
(5) Ghosh, P.; Garzione, C. N.; Eiler, J. M. *Science* **2006**, *311* (5760), 511−515.
(6) Huntington, K. W.; Lechler, A. R. *Tectonophysics* **2015**, *647−648*, 1−20.
(7) Halevy, I.; Fischer, W. W.; Eiler, J. M. *Proc. Natl. Acad. Sci. U. S. A.* **2011**, *108* (41), 16895−16899.
(8) Mangenot, X.; Gasparrini, M.; Gerdes, A.; Bonifacie, M.; Rouchon, V. *Geology* **2018**, *46* (12), 1067−1070.
(9) Pagel, M.; Bonifacie, M.; Schneider, D. A.; Gautheron, C.; Brigaud, B.; Calmels, D.; Cros, A.; Saint-Bezar, B.; Landrein, P.; Sutcliffe, C.; Davis, D.; Chaduteau, C. *Chem. Geol.* **2018**, *481*, 1−17.
(10) Saenger, C.; Affek, H. P.; Felis, T.; Thiagarajan, N.; Lough, J. M.; Holcomb, M. *Geochim. Cosmochim. Acta* **2012**, *99*, 224−242.
(11) Eagle, R. A.; Eiler, J. M.; Tripati, A. K.; Ries, J. B.; Freitas, P. S.; Hiebenthal, C.; Wanamaker, A. D.; Taviani, M.; Elliot, M.; Marenssi, S.; Nakamura, K.; Ramirez, P.; Roy, K. *Biogeosciences* **2013**, *10* (7), 4591−4606.
(12) Eagle, R. A.; Tütken, T.; Martin, T. S.; Tripati, A. K.; Fricke, H. C.; Connely, M.; Cifelli, R. L.; Eiler, J. M. *Science* **2011**, *333* (6041), 443−445.
(13) Huntington, K. W.; Eiler, J. M.; Affek, H. P.; Guo, W.; Bonifacie, M.; Yeung, L. Y.; Thiagarajan, N.; Passey, B.; Tripati, A.; Daëron, M.; Came, R. *J. Mass Spectrom.* **2009**, *44* (9), 1318−1329.
(14) Dennis, K. J.; Affek, H. P.; Passey, B. H.; Schrag, D. P.; Eiler, J. M. *Geochim. Cosmochim. Acta* **2011**, *75* (22), 7117−7131.
(15) Spencer, C.; Kim, S. T. *Geosci. J.* **2015**, *19* (2), 357−374.
(16) Bernasconi, S. M.; Müller, I. A.; Bergmann, K. D.; Breitenbach, S. F. M.; Fernandez, A.; Hodell, D. A.; Jaggi, M.; Meckler, A. N.; Millan, I.; Ziegler, M. *Geochem., Geophys., Geosyst.* **2018**, *19* (9), 2895−2914.
(17) Daëron, M.; Blamart, D.; Peral, M.; Affek, H. P. *Chem. Geol.* **2016**, *442*, 83−96.
(18) Schauer, A. J.; Kelson, J.; Saenger, C.; Huntington, K. W. *Rapid Commun. Mass Spectrom.* **2016**, *30* (24), 2607−2616.
(19) Tuzson, B.; Zeeman, M. J.; Zahniser, M. S.; Emmenegger, L. *Infrared Phys. Technol.* **2008**, *51* (3), 198−206.
(20) McManus, J. B.; Nelson, D. D.; Zahniser, M. S. *Opt. Express* **2015**, *23* (5), 6569−6586.

(21) Bergman, S. C.; Huntington, K. W.; Crider, J. G. *Am. J. Sci.* **2013**, *313* (5), 490−515.

(22) Steig, E. J.; Gkinis, V.; Schauer, A. J.; Schoenemann, S. W.; Samek, K.; Hoffnagle, J.; Dennis, K. J.; Tan, S. M. *Atmos. Meas. Tech.* **2014**, *7* (8), 2421−2435.

(23) Ono, S.; Wang, D. T.; Gruen, D. S.; Lollar, B. S.; Zahniser, M. S.; Mcmanus, J. B.; Nelson, D. D. *Anal. Chem.* **2014**, *86* (13), 6487−6494.

(24) Wang, D. T.; Gruen, D. S.; Lollar, B. S.; Hinrichs, K. U.; Stewart, L. C.; Holden, J. F.; Hristov, A. N.; Pohlman, J. W.; Morrill, P. L.; Könneke, M.; Delwiche, K. B.; Reeves, E. P.; Sutcliffe, C. N.; Ritter, D. J.; Seewald, J. S.; McIntosh, J. C.; Hemond, H. F.; Kubo, M. D.; Cardace, D.; Hoehler, T. M.; Ono, S. *Science* **2015**, *348* (6233), 428−431.

(25) Sakai, S.; Shimono, A.; Hikita, T.; McManus, J. B.; Zahniser, M. S.; Nelson, D. D.; Dettman, D. L. CO₂ Isotopologue Measurements of Carbonates by Tunable Mid-Infrared Laser Spectroscopy. In *Seventh International Symposium on Isotopomers*; Tokyo, Japan, 2014.

(26) Nelson, D.; Wang, Z.; Dettman, D.; Mcmanus, B.; Quade, J.; Huntington, K.; Schauer, A. Recent Progress towards Measuring the Clumped Isotopic Composition of Carbon Dioxide with Laser Spectroscopy. In *Seventh International Clumped Isotope Workshop*; Los Angeles, CA, 2019.

(27) Nelson, D.; Wang, Z.; Dettman, D.; Mcmanus, B.; Quade, J.; Huntington, K.; Schauer, A. Recent Progress towards Measuring the Clumped Isotopic Composition of Carbon Dioxide with Laser Spectroscopy. In *Geophysical Research Abstracts, EGU General Assembly 2019*; Vienna, Austria, 2019.

(28) Prokhorov, I.; Kluge, T.; Janssen, C. *Sci. Rep.* **2019**, *9*, 1−11.

(29) Sakai, S.; Matsuda, S.; Hikida, T.; Shimono, A.; McManus, J. B.; Zahniser, M.; Nelson, D.; Dettman, D. L.; Yang, D.; Ohkouchi, N. *Anal. Chem.* **2017**, *89* (21), 11846−11852.

(30) Wang, Z.; Schauble, E. A.; Eiler, J. M. *Geochim. Cosmochim. Acta* **2004**, *68* (23), 4779−4797.

(31) HITRAN. https://www.cfa.harvard.edu/hitran/.

(32) McManus, J. B.; Kebabian, P. L.; Zahniser, M. S. *Appl. Opt.* **1995**, *34* (18), 3336−3348.

(33) Nelson, D. D.; Shorter, J. H.; McManus, J. B.; Zahniser, M. S. *Appl. Phys. B: Lasers Opt.* **2002**, *75* (2−3), 343−350.

(34) Wacker, U.; Fiebig, J.; Schoene, B. R. *Rapid Commun. Mass Spectrom.* **2013**, *27* (14), 1631−1642.

(35) Petersen, S. V.; Defliese, W. F.; Saenger, C.; Daëron, M.; Huntington, K. W.; John, C. M.; Kelson, J. R.; Bernasconi, S. M.; Colman, A. S.; Kluge, T.; Olack, G. A.; Schauer, A. J.; Bajnai, D.; Bonifacie, M.; Breitenbach, S. F. M.; Fiebig, J.; Fernandez, A. B.; Henkes, G. A.; Hodell, D.; Katz, A.; Kele, S.; Lohmann, K. C.; Passey, B. H.; Peral, M. Y.; Petrizzo, D. A.; Rosenheim, B. E.; Tripati, A.; Venturelli, R.; Young, E. D.; Winkelstern, I. Z. *Geochem., Geophys., Geosyst.* **2019**, *20* (7), 3495−3519.

(36) Kelson, J. R.; Huntington, K. W.; Schauer, A. J.; Saenger, C.; Lechler, A. R. *Geochim. Cosmochim. Acta* **2017**, *197*, 104−131.